J Fail. Anal. and Preven. (2021) 21:472–487
https://doi.org/10.1007/s11668-020-01084-5

TECHNICAL ARTICLE—PEER-REVIEWED

Influence of Punch Velocity on Deformation Behavior in Deep Drawing of Aluminum Alloy

Yogesh Dewang · Vipin Sharma · Yash Batham

Submitted: 2 August 2020 / in revised form: 27 October 2020 / Accepted: 10 November 2020 / Published online: 25 November 2020

Abstract Deep drawing is one of the important sheet-forming processes. Several process parameters are responsible for producing defect-free products of deep drawing. Out of those parameters, blank holder force is one of the widely studied process parameters, which significantly influence deep drawing. In the present study, the effect of velocity of the punch on deformation behavior of aluminum alloys is investigated. FEM simulation is conducted using commercially available software ABAQUS. It is found through FEM simulation that effective stress increases by nearly 56% with an increment in punch velocity from 150 to 350 mm/s. Besides this, equivalent plastic strain increases by five times on increment in punch velocity from 150 to 350 mm/s. von Mises stress and equivalent plastic strain found to be maximum at flange radii region (die corner) at all velocities of punch. Wrinkling is found to be absent during deformation (loading step) at all punch velocities. Wrinkling is obtained in deep drawn cups after unloading of the punch at all punch velocities except the lowest velocity of 150 mm/s. The phenomenon of wrinkling was found to be pronounced with increment in velocity of the punch after unloading of the punch. For prevention of wrinkling tendency during deep drawing, the velocity of punch should be less than 200 mm/s. Besides this, punch force, effective stress, and equivalent plastic strain found to increase nonlinearly due to increment in punch stroke. It is gathered through FEM simulation that wrinkling phenomenon increases with increment in punch velocity due to unloading of the punch during deep drawing.

Keywords Deep drawing · Punch · Velocity · Wrinkling · Aluminum alloy

Y. Dewang (✉) · Y. Batham
Department of Mechanical Engineering, Lakshmi Narain College of Technology, Bhopal, India
e-mail: dewang.yogesh3@gmail.com

V. Sharma
Department of Mechanical Engineering, Sagar Institute of Research Technology and Science, Bhopal, India

Introduction

Deep drawing is a sheet metal-forming process in which a sheet is generally placed over an asymmetric die and deformed by a punch to produce cylindrical and circular cups. In such a sheet metal-forming process, drawing length of the part is higher than the diameter of the original sheet sample. Deep drawing has significance due to its industrial applications such as in manufacturing of light-weight components of cars as well as for cooking utensils. A number of crucial parameters in deep drawing greatly influence the deformation behavior of deep drawn parts.

Researchers in the past had focused on different regimes of the deep drawing process. Out of different regimes of deep drawing, researchers found blank holding forces found to be quite effective in understanding the deformation behavior of deep drawn components. Yoshihara et al. [1] recognized an improvement in limiting drawing ratio in deep drawing of magnesium alloy sheet due to the application of variable blank holding forces and asserted this improvement in limiting drawing ratio due to low values of strength coefficient. Lin et al. [2] integrated a new variable blank holding force strategy with PID closed-loop controller into the FEM simulation for the determination of variable blank holding force on segmental binders in sheet metal forming of aluminum alloys. Wifi and Mosallam [3]

implemented various unconventional schemes of blank holding forces such as friction-actuated blank holder, elastic blank holder, and pulsating blank holder forces for application in deep drawing. Kovac and Tittel [4] recommended the implementation of variable blank holding force instead of constant blank holding force to help in improvement of deep drawing as well as improvement in product quality due to optimization of blank holding forces. Zheng et al. [5] employed the macro-textured blank holders in hot deep drawing of aluminum alloys for the occurrence of flange wrinkling by considering a buckling model. Ozdilli et al. [6] recognized blank holder force to be a deciding factor responsible for the height of a drawn part; deep drawing height increases with blank holder force. Kumaravel and Venkatesh [7] found experimentally that wrinkling can be reduced by employing higher values of blank holding force while using relatively lower punch speed.

Besides this, it is also recognized by researchers that finite element simulation and experimentation are two important tools that greatly influence deep drawing process. In this context, researchers contributed to address the various aspects of deep drawing by using FEM and experiments. Wang et al. [8] utilized a multi-step FEM simulation methodology for obtaining the optimal blank shape for deep drawing of cups without ears, which can be applied to other stamping processes. Xue et al. [9] studied the twist springback characteristics of dual-phase steel sheet experimentally and through FEM simulation. Fazlollahi et al. [10] found that maximum drawing ratio is higher in case of hydro-mechanical deep drawing as compared to conventional deep drawing. Pepelnjak et al. [11] found increment in drawability of dual-phase steel by subjecting it to localized heating of the flange area in a temperature range of 473–573 K. Krachenfels et al. [12] investigated the effect of material properties of sheet in dry deep drawing by considering tribological conditions. Oleksik et al. [13] considered FEM simulation as an efficient methodology, which highlighted advantages such as better prediction of stress and strain as well as for better die design in deep drawing. Prakash et al. [14] determined the mechanical behavior of AA 5083 through biaxial tests and also conducted numerical simulation of deep drawing through flow curves obtained after uniaxial and biaxial tests. Panthi and Saxena [15] predicted the location of cracks in deep drawing using FEM simulation. The objective of the present study is to understand the influence of punch velocity on deformation behavior of AA 1100-O

Table 1 Details of geometrical parameters of deep drawing

S.No.	Geometrical parameters	Intensity
1	Initial blank thickness (mm)	1
2	Diameter of punch (mm)	40
3	Diameter of die (mm)	44
4	Diameter of blank (mm)	80
5	Drawing ratio	2

Table 2 Mechanical properties of AA 1100-O [15]

S.No.	Mechanical properties	Magnitude	Unit
1	Mass density	2710	kg/m^3
2	Modulus of elasticity	70	GPa
3	Poisson's ratio	0.33	NA
4	Strength coefficient	179	MPa
5	Work hardening coefficient	0.26	NA
6	Tensile yield strength	96	MPa

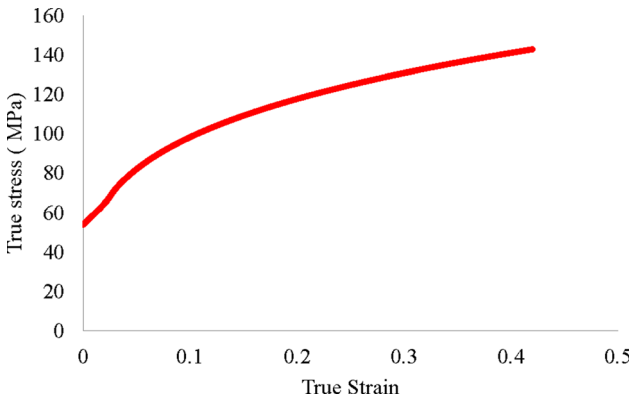

Fig. 1 True stress vs. true strain relationship for AA 1100-O [15]

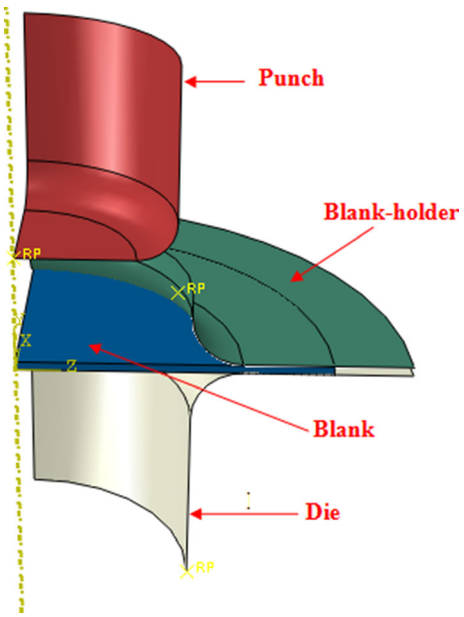

Fig. 2 Assembled CADD model of deep drawing

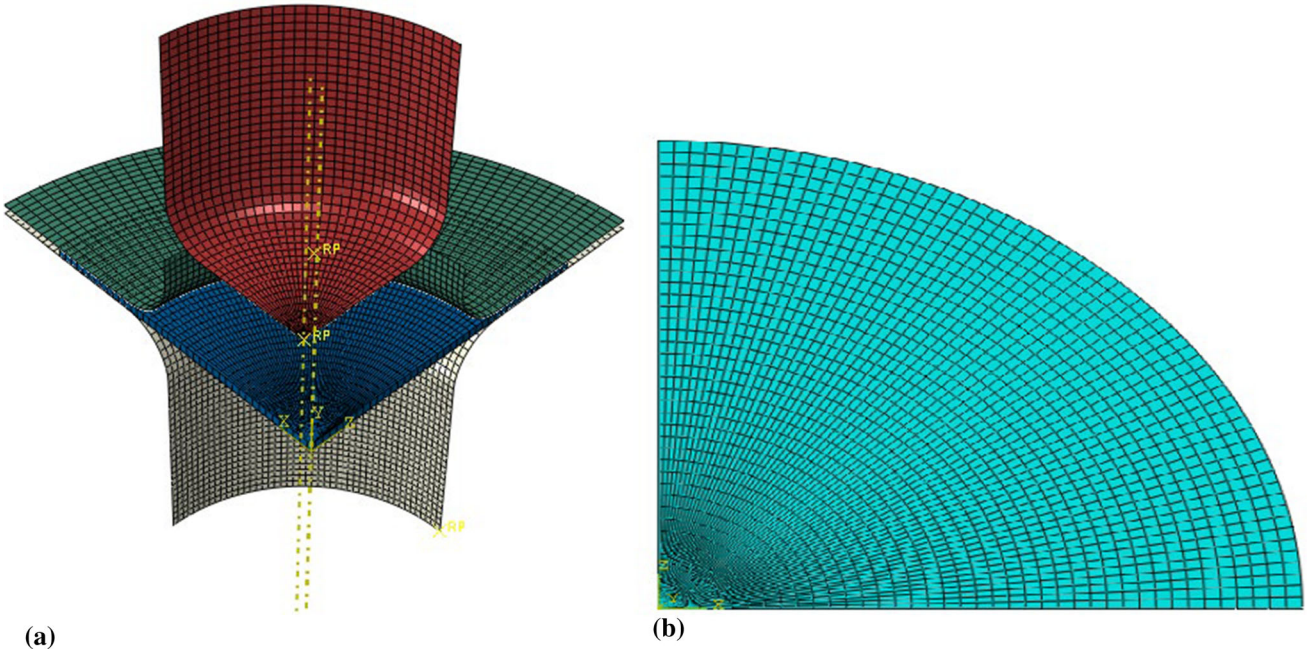

Fig. 3 FEM model and meshes of deep drawing: (**a**) combined model of mesh parts and (**b**) meshing of blank

Table 3 Description of element type, number of nodes, degrees of freedom and characteristics

S. No.	Name of component	Element type	Number of nodes	Degrees of freedom	Characteristics
1	Die	R3D4	4	3 translational degree of freedom per node (u_x, u_y,u_z)	Rigid element
2	Punch				
3	Blank holder				
4	Blank	C3D8R	8	3 translational degree of freedom per node (u_x, uy,u_z,)	Hexahedral solid element

Table 4 Meshing details of FEM model with number of nodes and elements

S. No.	Name of parts	Element type	Elements	Nodes
1.	Blank holder	R3D4	1692	1776
2.	Die	R3D4	2632	2736
3.	Punch	R3D4	1218	1291
3.		R3D3	29	
4.	Sheet	C3D8R	2457	5122
		C3D6	63	

Table 5 Details of FEM model with element type, element shape, and geometric order

S.No.	Element type	Element shape	Geometric order	Elements
1.	R3D4	Quadrilateral	Linear	5542
2.	R3D3	Triangular	Linear	29
3.	C3D8R	Hexahedral	Linear	2457
4.	C3D6	Wedge	Linear	63
				64

sheet metal of 1.0 mm thickness under deep drawing using FEM simulation.

Materials' Behavior

Aluminum alloy 1100-O is selected as the workpiece material in the present work by referring to the literature available. Isotropic hardening law is considered during FEM simulation. Material behavior is governed by power law relationship:

$$\sigma = K\varepsilon^n \quad \text{(Eq 1)}$$

where σ true stress in MPa, K strength coefficient in MPa, ε true strain, n strain hardening exponent.

Table 1 shows the geometrical details of the deep drawing process for the preparation of CADD model. Table 2 shows the material properties referred from Panthi and Saxena et al. [15] are used as inputs for FEM

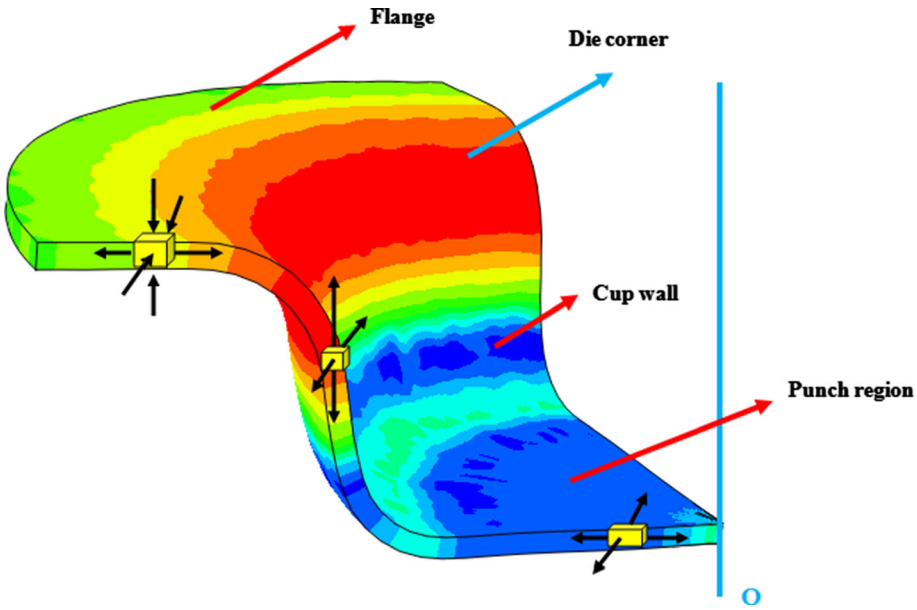

Fig. 4 Stresses and deformation in a section from a drawn cup

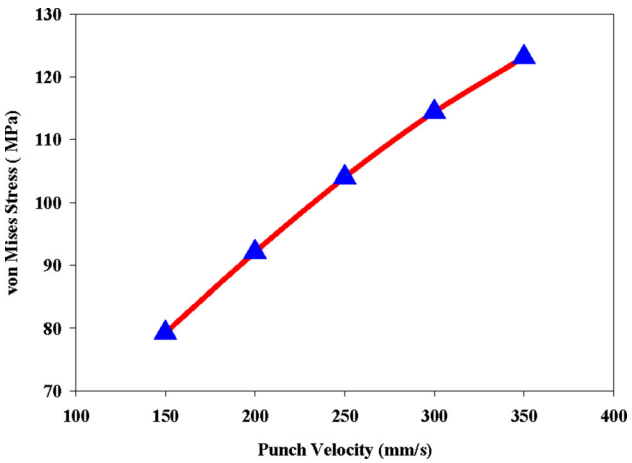

Fig. 5 Effect of punch velocity on von Mises stress

simulation here of deep drawing process. Figure 1 shows the true stress versus true strain behavior of AA-1100-O sheets.

Finite Element Simulation and Modeling

Axisymmetric CAD models of the punch, blank, blank holder, and die were prepared of required dimensions in the ABAQUS/CATIA-based module. Material is prepared virtually in the ABAQUS/CAE environment by assigning different material properties of aluminum alloy AA-1100-O considering isotropic hardening behavior governed by the power law. Assembly of tooling elements such as die, punch, and blank holder with sheet metal blanks was done, and it is clearly represented in Fig. 2. Two different steps were constructed for the whole FEM simulation of the deep drawing process. In the first step, the punch was given velocity to obtain the deformation of the sheet into a cylindrical cup, while blank holder and die remain fixed during this step. In the second step, the blank holder as well as punch was given velocity to move in the upward direction, but die remains fixed in this step too. Coefficient of friction was chosen for interaction between the three sets of interacting surfaces. Contact was between different interacting surfaces, i.e., between punch and sheet (μ_{ps} = 0.1), die and sheet (μ_{ds} = 0.05), blank holder and sheet (μ_{bs} = 0.08). Surface-to-surface contact with penalty contact formulation was utilized and assigned with different coefficients of friction for contact during forming. The sheet blank was considered as a deformable entity, and aluminum alloy AA-1100-O was assigned to form a solid homogenous section to be utilized for deep drawing. Figure 3a shows the meshed FEM model of deep drawing process. Meshing of the sheet metal blanks was conducted using a three-dimensional solid continuum eight-noded brick element type (C3D8R) and is shown in Fig. 3b. Tooling elements such as punch, die, and blank holder were modeled as discrete rigid elements and were discretized with 4-node 3-D bilinear rigid quadrilaterals. Table 3 gives the details of the element type used and degree of freedom involved for different parts of FEM model. Table 4 gives the detailed description of meshing

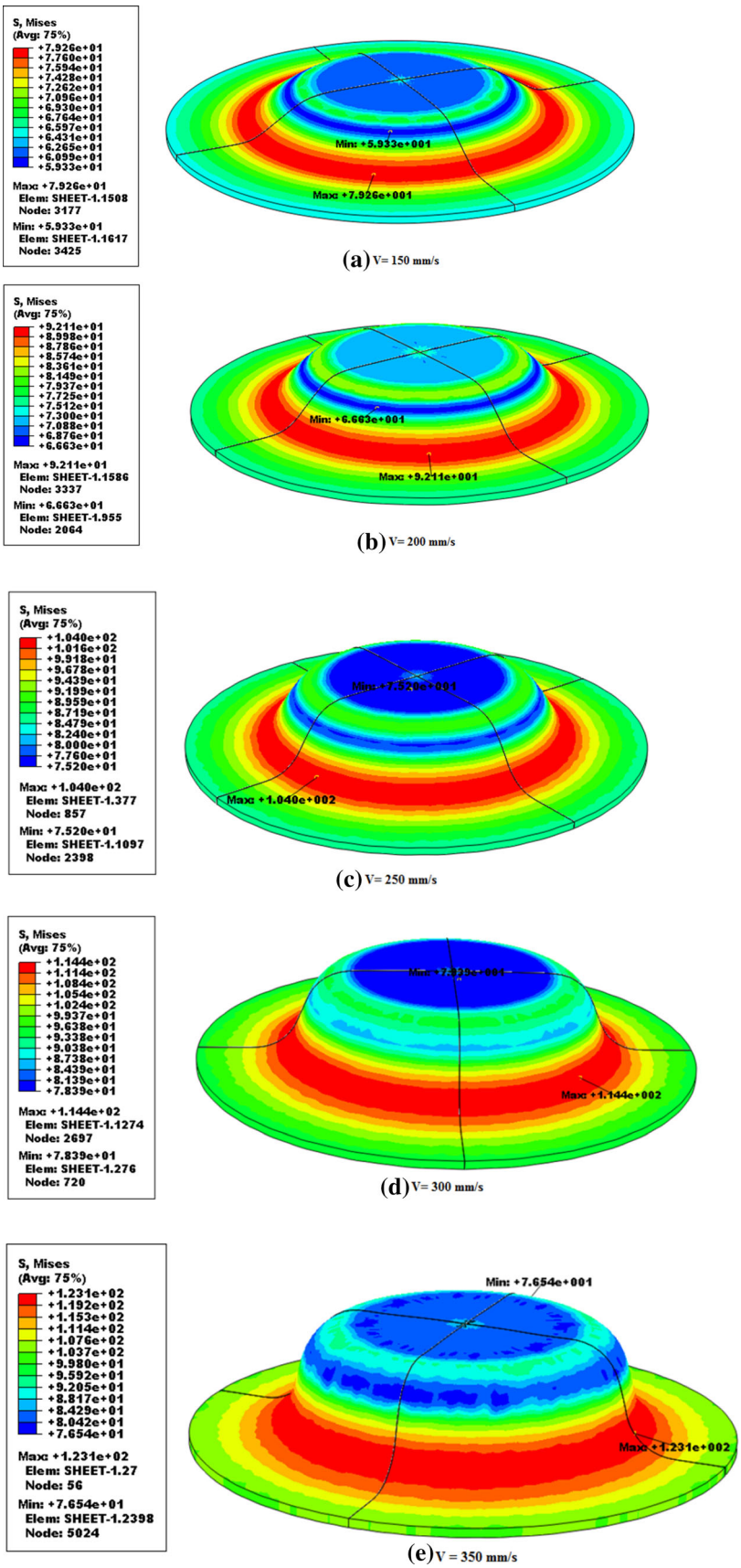

Fig. 6 Contour plots of von Mises stress distribution for different punch velocities

Table 6 Location of maximum von Mises stress (σ_{max}) and maximum equivalent plastic strain (ε_{max})

S.No.	Velocity (mm/s)	Location of (σ_{max}) after loading step	Location of (σ_{max}) after unloading step	Location of (ε_{max}) after loading	Location of (ε_{max}) after unloading
1	150	Flange profile radii (die corner)	Flange profile radii (die corner)	Flange profile radii (die corner)	Flange profile radii (die corner)
2	200	Flange profile radii (die corner)	Flange profile radii (die corner)	Flange profile radii (die corner)	Flange profile radii (die corner)
3	250	Flange profile radii (die corner)	Flange profile radii (die corner)	Flange profile radii (die corner)	Flange profile radii (die corner)
4	300	Flange profile radii (die corner)	Flange profile radii (die corner)	Flange profile radii (die corner)	Flange profile radii (die corner)
5	350	Flange profile radii (die corner)	Flange profile radii (die corner)	Flange profile radii (die corner)	Flange profile radii (die corner)

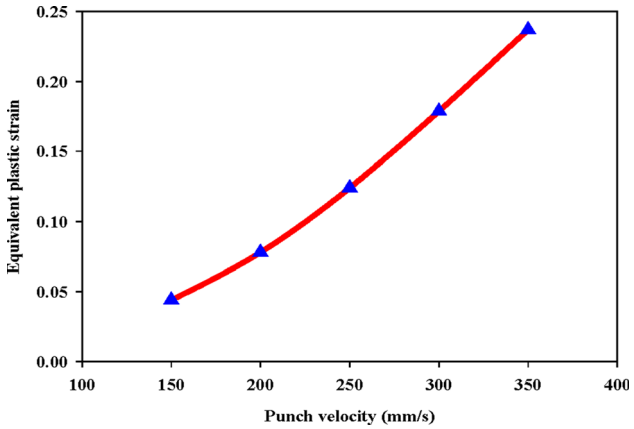

Fig. 7 Effect of punch velocity on equivalent plastic strain

details with number of elements and nodes in FEM-meshed model of deep drawing. Geometric order, element shape, and number of elements hold for different element types are given in Table 5. In the first step, all six degrees of freedom of die and blank holder were restrained to make both fixed during FEM simulation. Besides this, XSYMM and ZSYMM boundary conditions were applied on the sheet metal blank. The punch could move in the vertical direction, and other degrees of freedom remained constrained during simulation. After that, velocity was assigned to the punch for deep drawing of cups. In the second step, the die remains fixed and symmetry boundary conditions were imposed on the sheet metal blank. In this second step, unloading was executed such that the blank holder and punch were allowed to move in the upward direction, and after that, velocity was assigned to the punch and blank holder for their upward movement.

Results and Discussion

Effect of Punch Velocity on Effective (von Mises) Stress

Figure 4 shows the different zones of pie-shaped segment of circular blank after deep drawing, which comprises flange region, die corner, cup wall, and punch region. Three-dimensional state of stress is experienced in the flange region, in which tensile stress acts in the radial direction due to stretching of blank into die cavity, compressive stress acts in the normal direction due to compression imparted through blank holder, and finally compressive stress are generated in the circumferential direction owing to circumferential shrinkage and due to radial tensile stresses as well [16]. Bending occurs at the die radius, and then, straightening occurs at die wall which are subjected to tensile stresses too [16]. Plastic bending

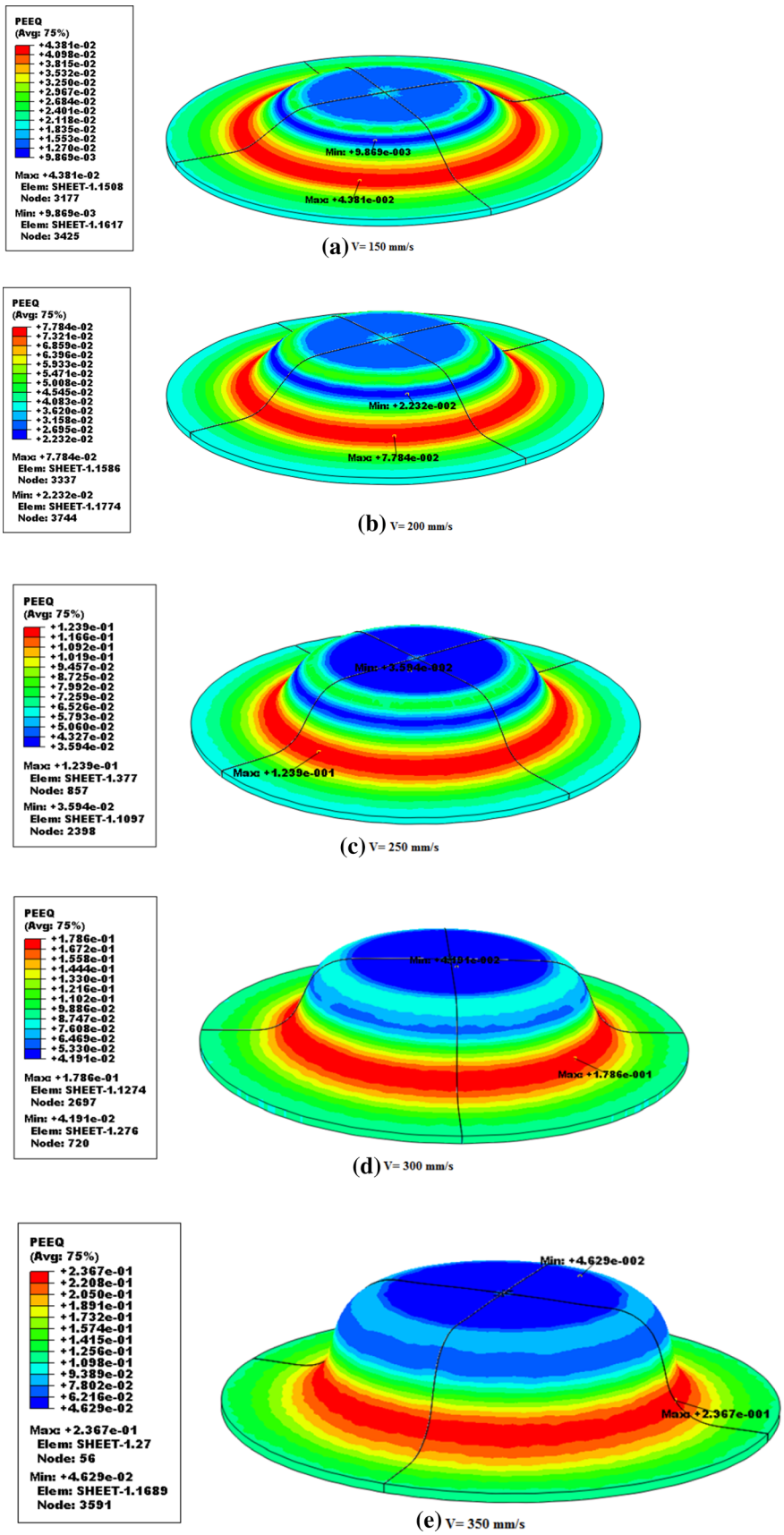

Fig. 8 Contour plots of equivalent plastic strain distribution for different punch velocities

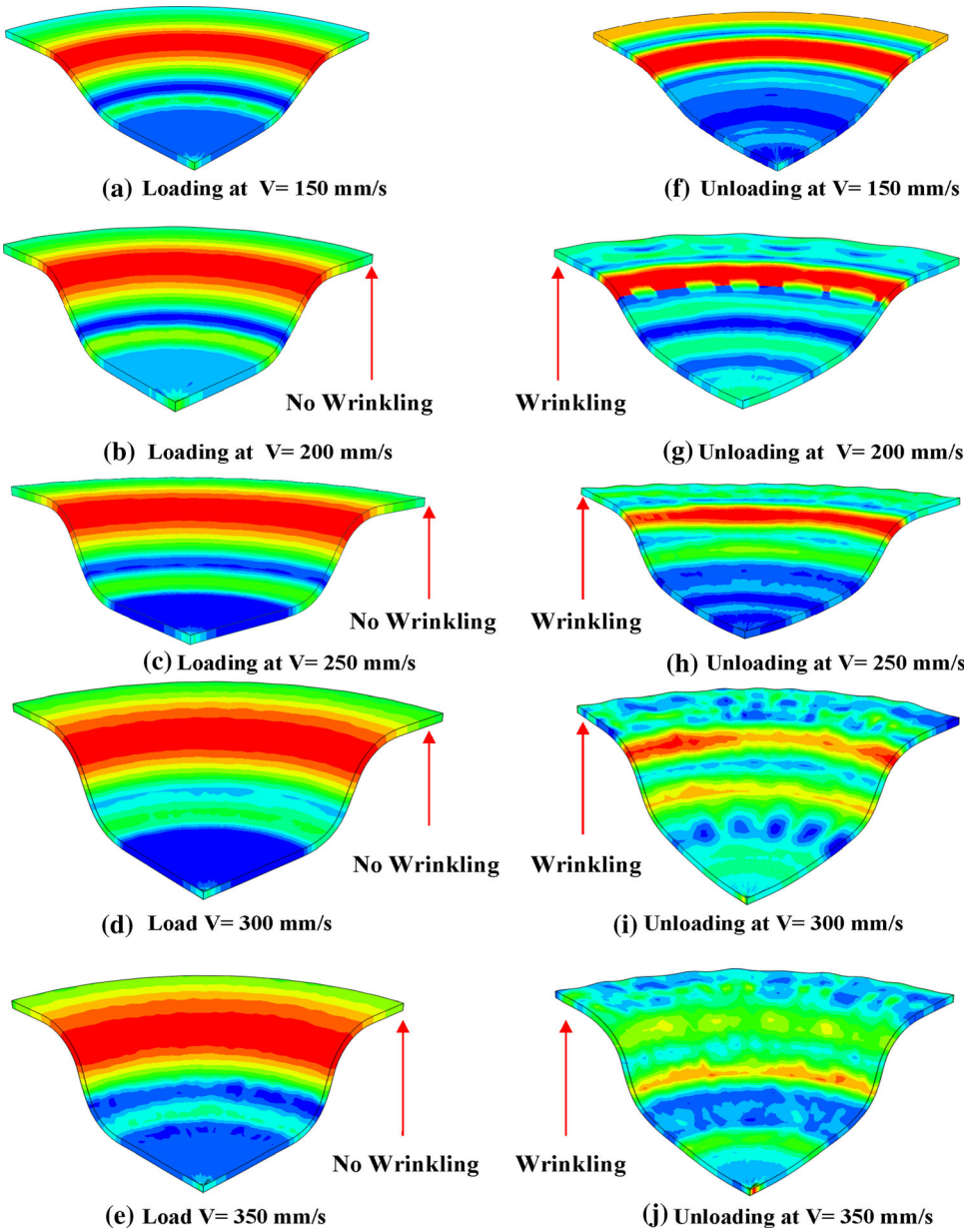

Fig. 9 Contour plots of maximum stress distribution (**a**–**e**) loading and (**f**–**j**) unloading steps

over the die radius through tension results in appreciable thinning, which alter the thickening due to shortening in the circumferential direction. A biaxial state of stresses is experienced by the cup wall as well as in the punch region, and both is tensile in nature [16]. Drawing force is transmitted by the punch via cup wall, and it is drawn into die via flange [16]. Circumferential stress in tensile nature is also generated through cup for firm holding over punch.

Figure 5 shows the variation of maximum effective stress (von Mises stress) due to the influence of punch velocity. It is found that von Mises stress increases more or less in a nonlinear manner. It is gathered from Fig. 5 that maximum von Mises stress increases by 55.3% on increasing the velocity of the punch from 150 to 350 mm/s (in steps of 50 mm/s). It can be seen clearly from Fig. 6 that von Mises stress distribution is different for five different cases of punch velocity. It is clear from Fig. 6 that maximum von Mises stress occurs at flange profile radii (die corner) for all velocities of punch both during loading and during unloading steps of deep drawing. This location of maximum von stress at the flange region (die corner) is also confirmed by Sahu and Pradhan [17]. Table 6 gives

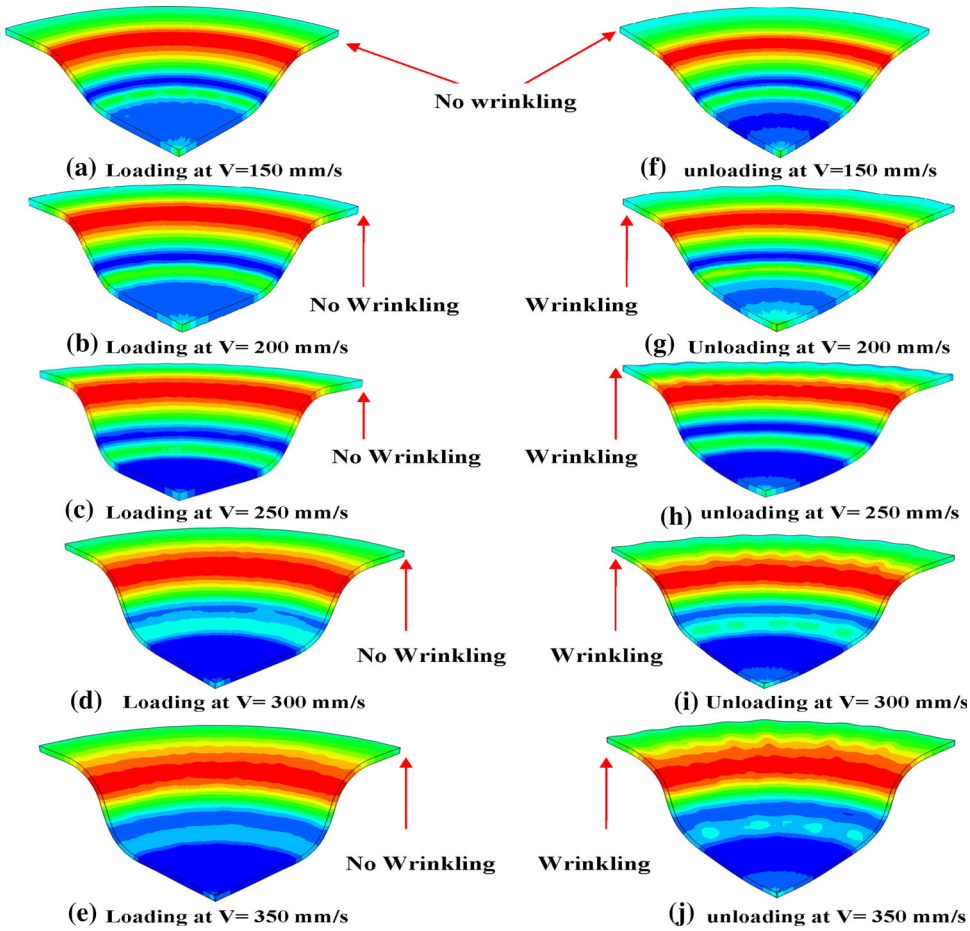

Fig. 10 Contour plots of equivalent plastic strain distribution (**a–e**) loading and (**f–j**) unloading steps

the location of maximum von Mises stress in the deep drawn cup due to the influence of punch velocity, i.e., at flange radii. It is clear from Fig. 6 that von Mises stress increases with increment in velocity. Maximum stress and maximum strain are developed at the highest velocity as well as due to maximum punch stroke. Effect of punch velocity and punch stroke leads to generation of higher von Mises stresses and equivalent plastic strain developed within deep drawn cup. Colgan and Monaghan [16] also proclaimed that higher speed leads to greater depth of deep drawing. A similar trend is found by Ju et al. [18], which revealed that higher forming speed leads to higher depth of deep drawn cup, which in turn leads to generation of maximum stresses within deep drawn cup. It is seen that both maximum von stress and maximum-induced plastic strain increased due to the effect of the velocity of punch, since in turn it increased the drawn height of cup simultaneously during deep drawing. In nut shell, both velocity of punch and punch stroke lead to peak stress and peak strain in deep drawing.

Effect of Punch Velocity on Equivalent Plastic Strain

Figure 7 shows the variation of equivalent plastic strain due to the influence of punch velocity. It is found that equivalent plastic strain increases in a nonlinear manner. It is found from Fig. 7 that equivalent plastic strain increased nearly by five times upon increasing the velocity of the punch from 150 to 350 mm/s (in steps of 50 mm/s). It is seen from Fig. 8 that equivalent plastic strain distributions are different for five different cases of punch velocity. It is clear from Fig. 8 that the location of maximum equivalent plastic strain is obtained at die corner near flange radii for all cases due to the effect of velocity of punch. Besides this,

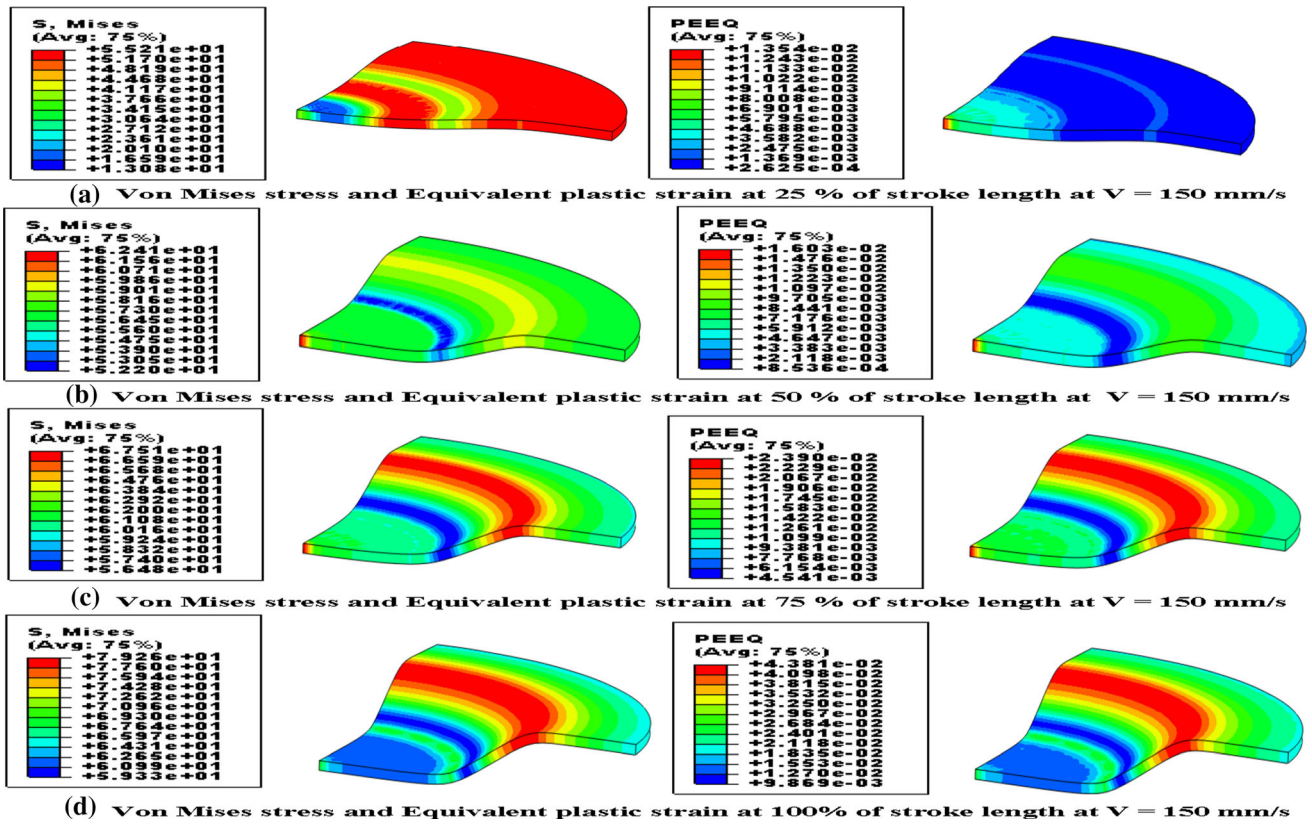

Fig. 11 Contour plots of von Mises stress and equivalent plastic strain at various stroke lengths and V = 150 mm/s

in another analysis of sheet metal forming, Akinlabi and Akinlabi [19] found that induced plastic strain increased with increased punch stroke. Table 6 gives the location of maximum equivalent plastic strain in the deep drawn cup due to the influence of punch velocity. The location of maximum equivalent plastic strain is found to be at the flange profile radii for all punch velocities. In summary, equivalent plastic strain is found to be influenced by punch velocity as well as by punch stroke length.

Comparison of von Mises Stress After Loading and Unloading Steps at Different Velocities of Punch

The location of maximum von Mises stress after loading and unloading steps of deep drawing is given in Table 6, i.e., at flange radii (die corner) in majority of cases. Maximum von Mises stress increases continuously with increment in velocity of the punch during the loading step. Figure 9 shows the distribution of von Mises stress after both the loading step and unloading step, which clearly depicts that there will be no wrinkling in the deep drawn cup in any of the cases due to punch velocity. Wrinkling phenomenon was observed after the unloading step in the cases for the punch velocity in the range from V = 200 mm/s to V = 350 mm/s due to the upward movement of punch. No wrinkling was observed in deep drawn cup after unloading of punch at the lowest punch velocity = 150 mm/s. Maximum von Mises stress increased continuously with increment in velocity of punch after both loading and unloading steps.

Comparison of Equivalent Plastic Strain After Loading and Unloading Steps at Different Velocities of Punch

Location of maximum equivalent plastic strain after loading and unloading steps of deep drawing is given in Table 6, i.e., at flange radii (die corner) in all cases. Maximum equivalent plastic strain increased continuously with increment in velocity of punch during the loading step. Figure 10 shows the distribution of equivalent plastic

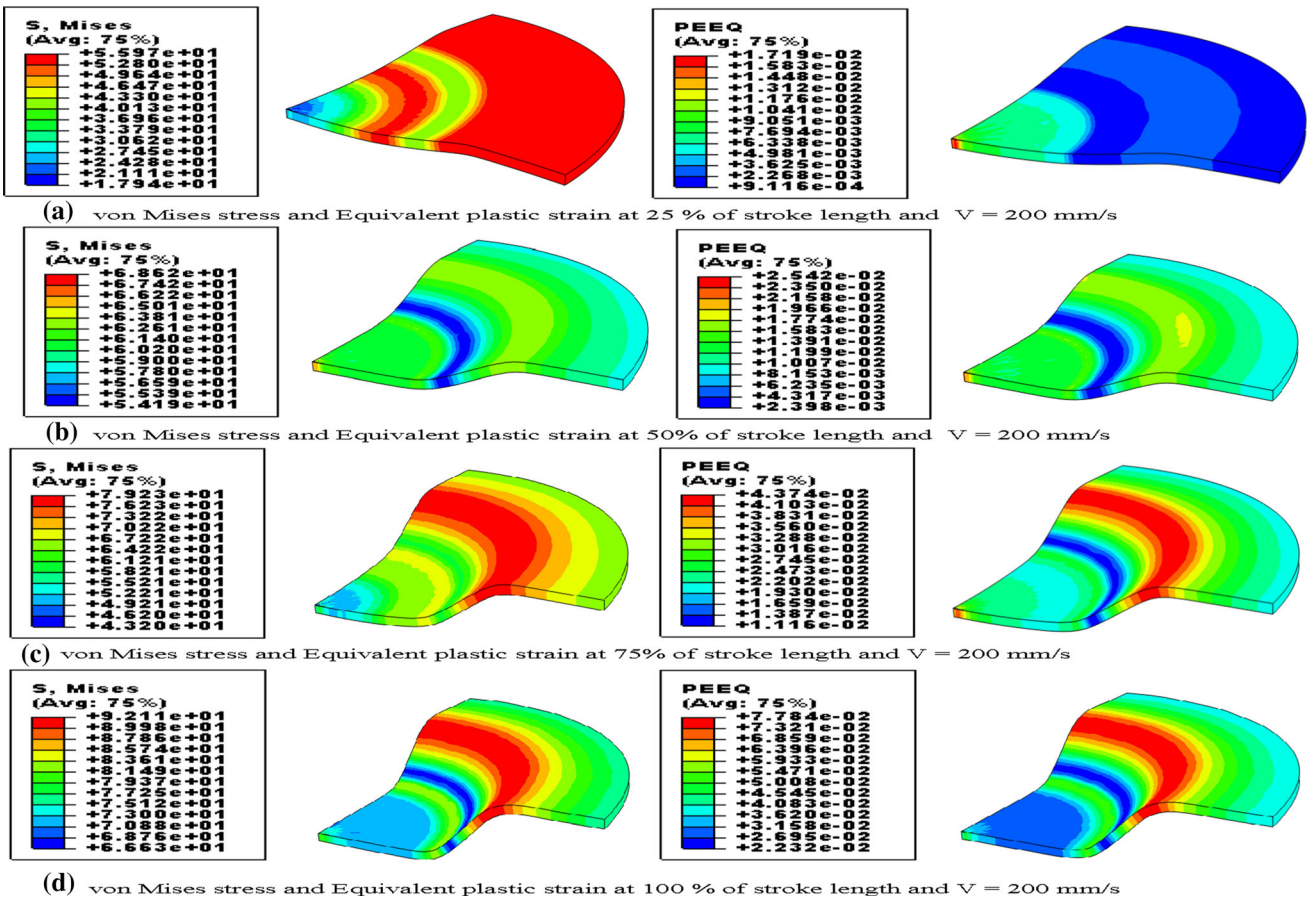

Fig. 12 Contour plots of von Mises stress and equivalent plastic strain at various stroke lengths and V = 200 mm/s

strain after both the loading step and the unloading step, which clearly depicts that there will be no wrinkling in the deep drawn cup in any of the cases due to punch velocity. Wrinkling phenomenon was observed after unloading step in the cases for the punch velocity in the range from V = 200 mm/s to V = 350 mm/s due to the upward movement of the punch. No wrinkling was observed in the deep drawn cups after unloading of the punch at the lowest punch velocity = 150 mm/s. Maximum equivalent plastic strain increased continuously with increment in velocity of punch after both loading and unloading steps.

Effect of Punch Stroke (Punch Displacement)

Figures 11, 12, 13, 14, and 15 show the different contour plots of von Mises stress and equivalent plastic strain distribution because of punch stroke (punch displacement) at different velocities of punch. It is clear from the contour plots of von Mises stress and equivalent plastic strain that both these field variables increased due to increment in punch stroke length. It is also clear from Figs. 16 and 17 that both von Mises stress and equivalent plastic strain increase nonlinearly with the increase in punch stroke length. Besides this, Fig. 18 shows the variation of punch force with punch displacement obtained through FEM simulation. It is gathered from Fig. 18 that punch load increases with punch stroke length in a nonlinear manner for obtaining drawing depth in deep drawing of cylindrical cups. Punch force attains peak for maximum displacement of punch and then drops due to unloading step of punch. Higher punch force is obtained for peak velocities.

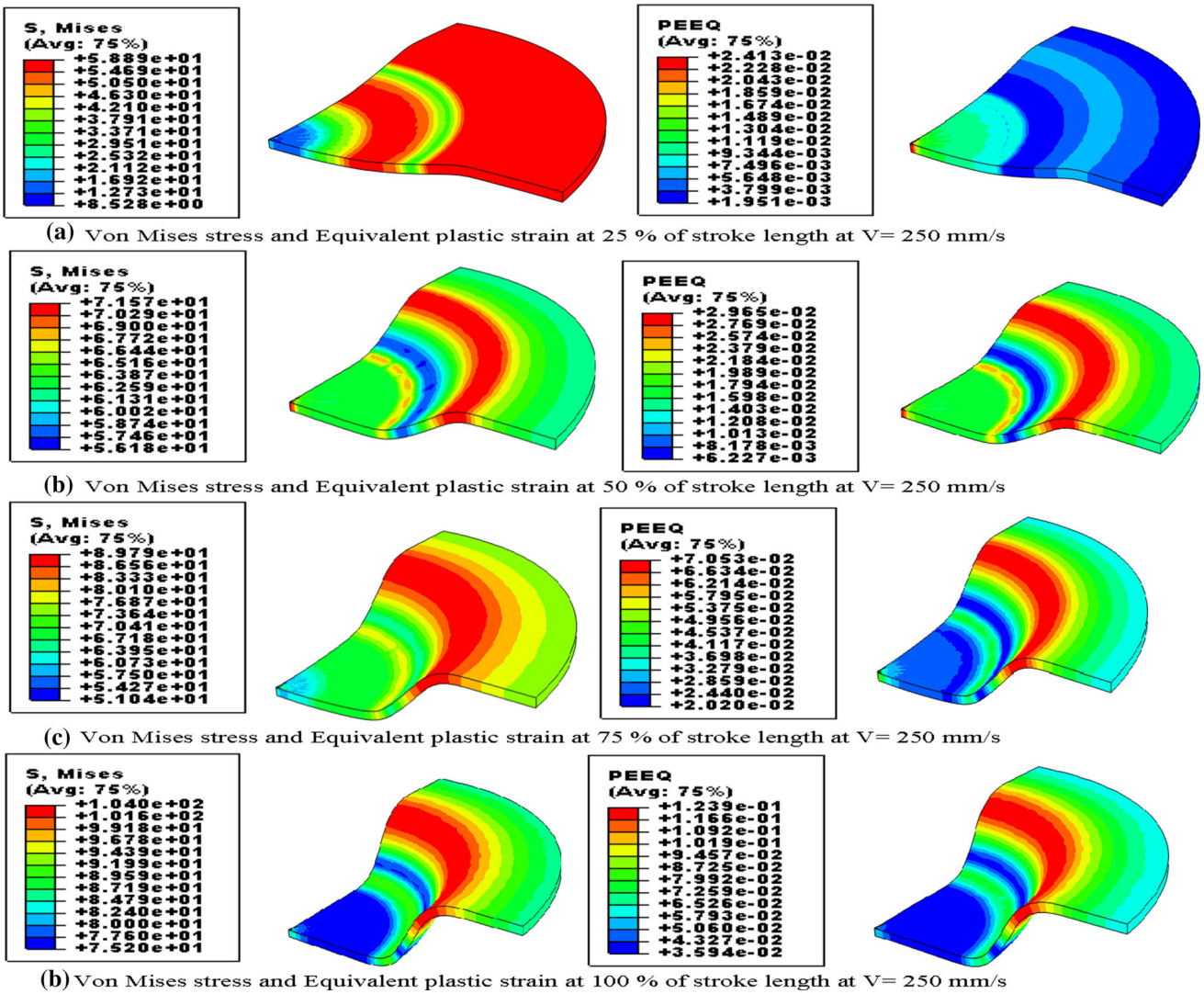

Fig. 13 Contour plots of von Mises stress and equivalent plastic strain at various stroke lengths and V = 250 mm/s

Conclusions

FEM simulation of the deep drawing process was conducted using AA-1100-O sheets using commercially available software package ABAQUS/6.14. The main objective of the present investigation was to evaluate the effect of velocity of the punch on deformation characteristics of cylindrical cups. The following are the conclusions drawn from the present study:

1. Effective stress increased by nearly 56% with increment in punch velocity from 150 to 350 mm/s.
2. Equivalent plastic strain increased by five times on increment in punch velocity from 150 to 350 mm/s.
3. von Mises stress and equivalent plastic strain found to be maximum at flange radii region (die corner) at all velocities of punch.
4. No clear evidence of wrinkling was found after the loading step due to increment in velocity of punch.

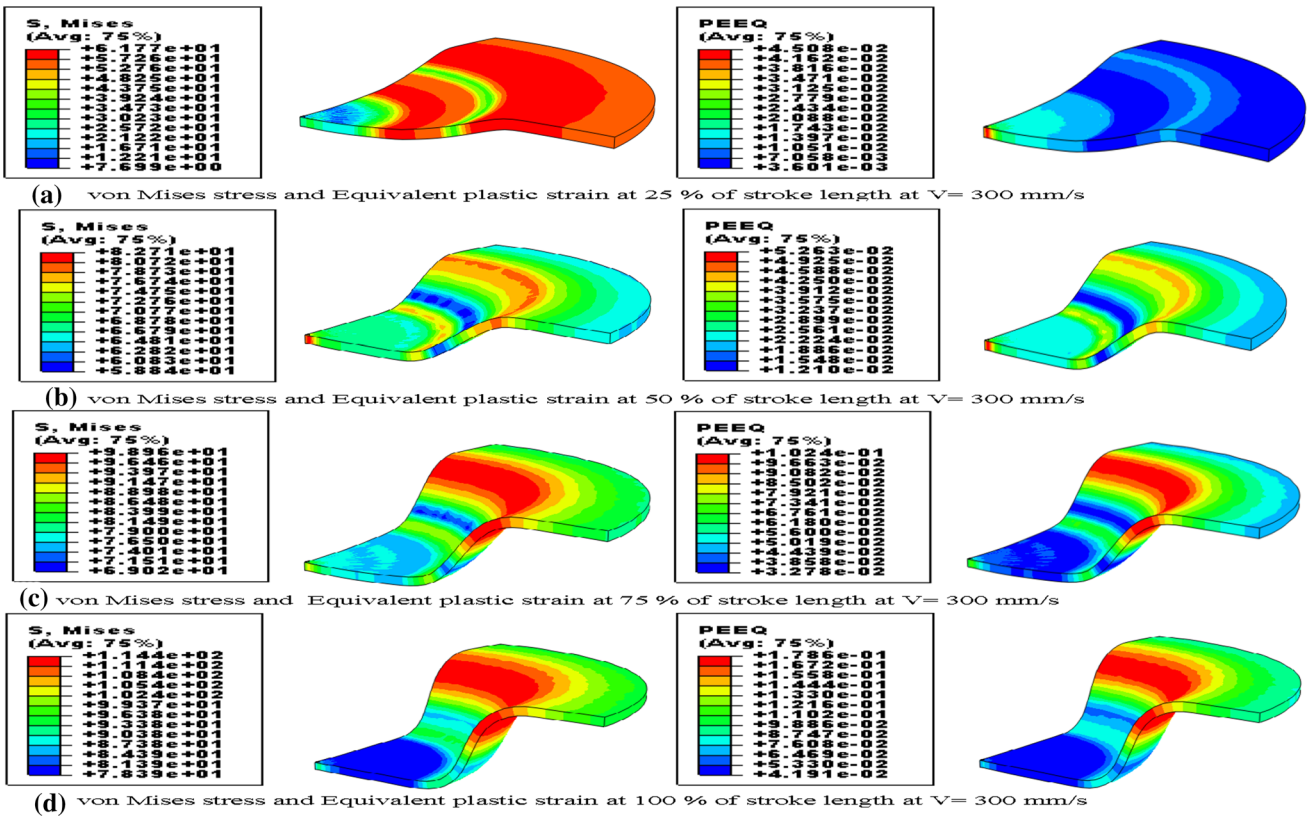

Fig. 14 Contour plots of von Mises stress and equivalent plastic strain at various stroke lengths and V = 300 mm/s

5. Wrinkling was absent at the lowest velocity of punch at 150 mm/s, while wrinkling was observed as a forming defect upon increment of velocity of the punch from 200 to 350 mm/s during unloading.
6. The phenomenon of wrinkling was found to be pronounced with increment in velocity of the punch after unloading of the punch. For prevention of wrinkling tendency during deep drawing, the velocity of punch should be less than 200 mm/s.
7. Punch force, effective stress, and equivalent plastic strain were found to be increased nonlinearly due to increment in punch stroke.

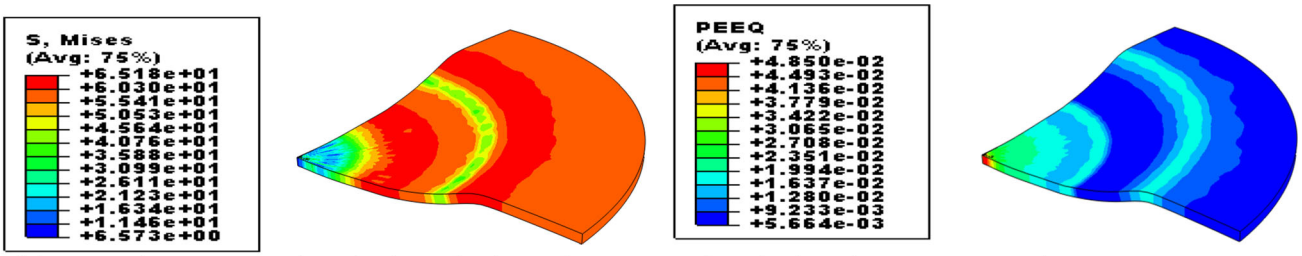

(a) von Mises stress and equivalent plastic strain at 25 % of stroke length at V= 350 mm/s

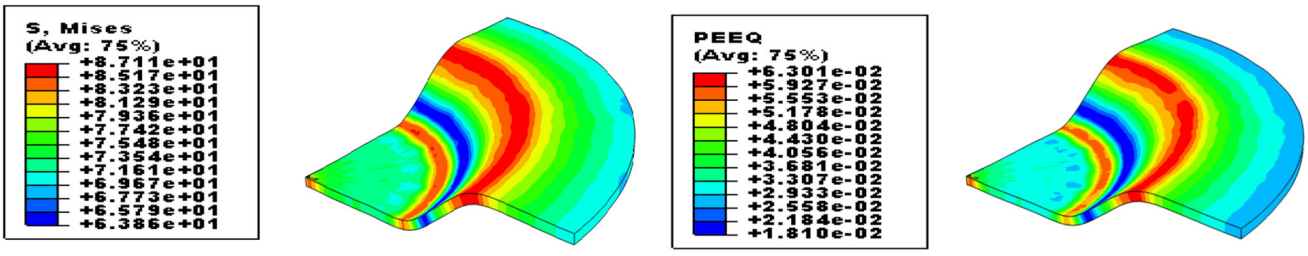

(b) von Mises stress and equivalent plastic strain at 50 % of stroke length at V= 350 mm/s

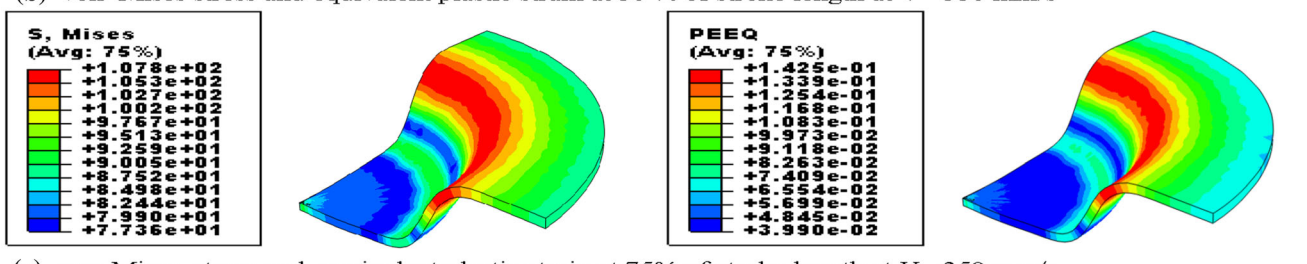

(c) von Mises stress and equivalent plastic strain at 75% of stroke length at V= 350 mm/s

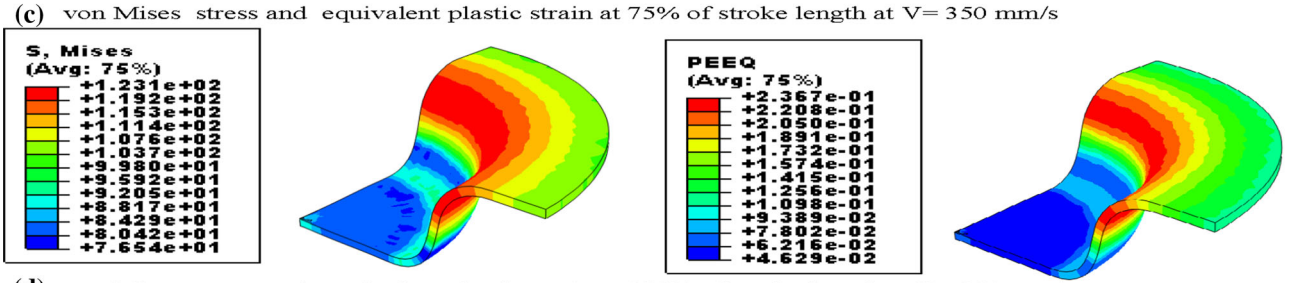

(d) von Mises stress and equivalent plastic strain at 100% of stroke length at V= 350 mm/s

Fig. 15 Contour plots of von Mises stress and equivalent plastic strain at various stroke lengths and V = 350 mm/s

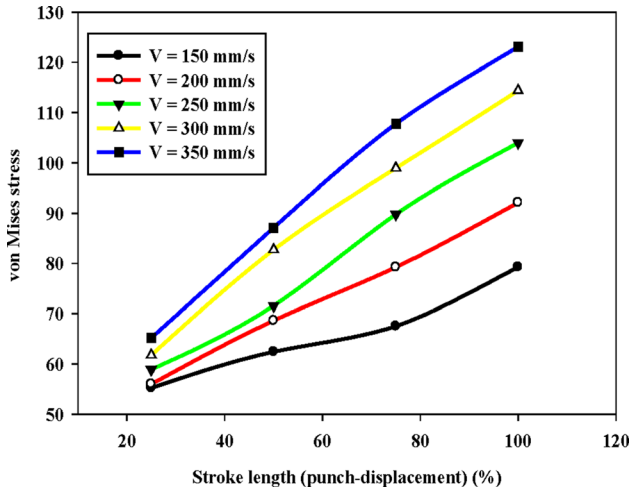

Fig. 16 Effect of punch stroke length on von Mises stress at different velocities of punch

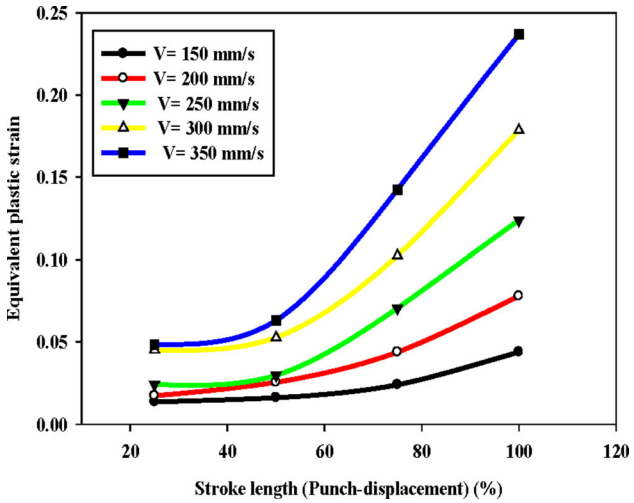

Fig. 17 Effect of punch stroke length on equivalent plastic strain at different velocities of punch

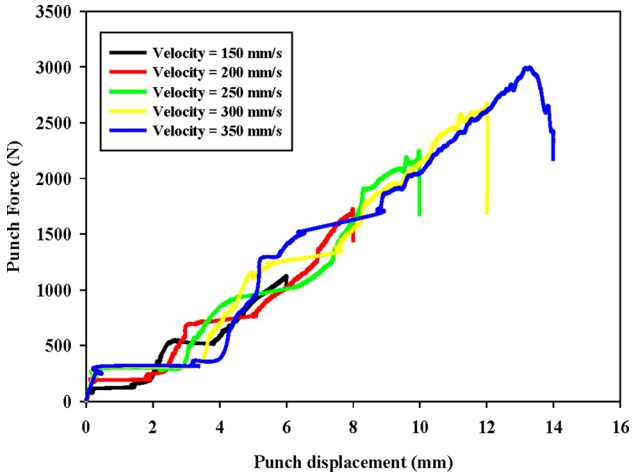

Fig. 18 Punch load vs. punch displacement curves for different velocities of punch

References

1. S. Yoshihara, K.I. Manabe, H. Nishimura, Effect of blank holder force control in deep-drawing process of magnesium alloy sheet. J. Mater. Process. Technol. **170**(3), 579–585 (2005)
2. L.Z. Qin, W.W. Rong, C.G. Long, A new strategy to optimize variable blank holder force towards improving the forming limits of aluminum sheet metal forming. J. Mater. Process. Technol. **183**(2–3), 339–346 (2007)
3. A. Wifi, A. Mosallam, Some aspects of blank-holder force schemes in deep drawing process. J. Achiev. Mater. Manuf. **24**(1), 315–323 (2007)
4. P. Kováč, V. Tittel, Blank holder force optimization of hemispherical product using numerical simulation. Mater. Sci. Technol. **5**, 5–10 (2010)
5. K. Zheng, J. Lee, J. Lin, T.A. Dean, A buckling model for flange wrinkling in hot deep drawing aluminium alloys with macro-textured tool surfaces. Int. J. Mach. Tools Manuf. **114**, 21–34 (2017)
6. O. Ozdilli, M.E. Erdin, M. Erdogan, Investigation of effects of variable blankholder force on deep drawing process of 6082 aluminum alloy. Fresenius Environ. Bull. **28**(4A), 3324–3332 (2019)
7. D. Kumaravel, K. Venkatesh, in *Reduction of Wrinkling Defect in Deep Drawing Process, Advances in Manufacturing Processes: Lecture Notes in Mechanical Engineering*, K.S. Vijay Sekar, M. Gupta, A. Arockiarajan, editors, February 15–16, 2018 (Chennai), Springer, Singapore, pp. 133–139 (2019)
8. J. Wang, A. Goel, F. Yang, J.T. Gau, Blank optimization for sheet metal forming using multi-step finite element simulations. Int. J. Adv. Manuf. **40**(7–8), 709–720 (2009)
9. X. Xue, J. Liao, G. Vincze, F. Barlat, Twist springback characteristics of dual-phase steel sheet after non-axisymmetric deep drawing. Int. J. Mater. Form. **10**(2), 267–278 (2017)
10. M. Fazlollahi, M.R. Morovvati, B.M. Dariani, Theoretical, numerical and experimental investigation of hydro-mechanical deep drawing of steel/polymer/steel sandwich sheets. Proc. Inst. Mech. Eng. B J. Eng. Manuf. **233**(5), 1529–1546 (2019)
11. T. Pepelnjak, E. Kayhan, B. Kaftanoglu, Analysis of non-isothermal warm deep drawing of dual-phase DP600 steel. Int. J. Mater. Form. **12**(2), 223–240 (2019)
12. K. Krachenfels, B. Rothammer, R. Zhao, S. Tremmel, M. Merklein, Influence of varying sheet material properties on dry deep drawing process, June (3–7), 2019, in *IOP Conference Series: Materials Science and Engineering*, p. 012012 (2019)
13. V. Oleksik, R. Breaz, G. Racz, P.D. Brindasu, O. Bologa, Advanced techniques used in numerical simulation for deep-drawing process, in *MATEC Web of Conferences 2019 9th International Conference on Manufacturing Science and Education, Sibiu, Romania* (2019)
14. V. Prakash, D.R. Kumar, A. Horn, H. Hagenah, M. Merklein, Modeling material behavior of AA5083 aluminum alloy sheet using biaxial tensile tests and its application in numerical simulation of deep drawing. Int. J. Adv. Manuf. **106**(3–4), 1133–1148 (2020)
15. S.K. Panthi, S. Saxena, Prediction of crack location in deep drawing processes using finite element simulation. Comput. Mater. Contin. **32**(1), 15–27 (2012)
16. M. Colgan, J. Monaghan, Deep drawing process: analysis and experiment. J. Mater. Process. Technol. **132**(1–3), 35–41 (2003)
17. Y.K. Sahu, M.K. Pradhan, in *Modelling and Simulation of Deep Drawing Process of Circular Cup on AL1200 Using Finite Element Analysis, Advances in Simulation, Product Design and Development: Lecture Notes on Multidisciplinary Industrial Engineering Book Series*, M.S. Shunmugam, M. Kanthababu,

editors, December 13–15, 2018 (Chennai), Springer, Singapore, pp. 29–42 (2019)
18. L. Ju, T. Mao, S. Patil, T. Altan, Investigation of forming speed and friction on drawability of Al 5182-O using a servo press with CNC cushion, Center for Precision Forming, The Ohio State University, Columbus, USA, Promotional Literature, Undated
19. S. Akinlabi, E. Akinlabi, Effect of punch stroke on deformation during sheet forming through finite element, July (3–4), 2017, in *IOP Conference Series: Materials Science and Engineering*, p. 012004 (2017)